IEEE Access
Multidisciplinary : Rapid Review : Open Access Journal

Received September 8, 2018, accepted September 24, 2018, date of publication October 25, 2018, date of current version November 30, 2018.

Digital Object Identifier 10.1109/ACCESS.2018.2878046

Design of an Online Nonlinear Optimal Tracking Control Method for Unmanned Ground Systems

JIE LIU[1], WEI HAN[1], YONG ZHANG[1], ZHIGANG CHEN[2], AND HAIJUN PENG[3]
[1]Naval Aeronautical and Astronautical University, Yantai 264001, China
[2]China Aerodynamics Research and Development Center, Mianyang 621000, China
[3]Dalian University of Technology, Dalian 116024, China
Corresponding author: Jie Liu (liuyexiaobao@163.com)

ABSTRACT A nonlinear tracking error model for unmanned ground systems (UGS) was developed, and the constraints and objective function were established; the tracking control problem for UGS was converted to a continuous nonlinear optimal control problem. In order to solve the complex problem, a symplectic pseudospectral method based on the third kind of generation function is proposed. This approach largely reduces the sensitivity of the initial guess for costate variables, and the characteristics of the original system are not lost after discretization, which is not the case for other methods. Subsequently, by considering the influences of random disturbances in the environment, the symplectic pseudospectral method and the receding horizon control principle are combined to solve the nonlinear tracking problem; this method overcomes the problem that a nonlinear optimal control method is difficult to apply for online tracking. Finally, the proposed method is verified using simulation experiments, and it is demonstrated that the proposed method achieves online and real-time tracking control of a standard trajectory in the presence of random disturbances and it provides great maneuverability and feasibility for practical applications.

INDEX TERMS Optimal control, nonlinear control systems, mathematical programming.

I. INTRODUCTION

Recently, unmanned ground systems (UGS), including ground transport of unmanned aerial vehicles (UAV), unmanned vehicles and robots, has been widely used in the aerospace, military, civil and other fields and an increasing number of research studies on UGS are being conducted [1]. The most important control problems of UGS include positioning, path planning, and trajectory tracking [2]. Trajectory tracking is a key issue that allows the UGS to move according to a given standard path (or reference path). However, there are still critical issues in trajectory tracking that are difficult to solve and they include (1) the nonlinear and coupled characteristics of the system, (2) the physical constraints of the control input and output, and (3) the impact of uncertainties in the environment [3], [4].

In order to solve these problems, the original nonlinear system is commonly converted into a linear time-varying/time-invariant system by using a linearization method and the controller is designed to implement the tracking task using linear control theory. Falcone *et al.* [5], [7] and Borrelli [6] proposed a model predictive control (MPC) method based on a continuous online linearization of nonlinear vehicle models. Kühne *et al.* [8] used the linear MPC for the linearization of an error model for a wheeled mobile robot (WMR), and proposed an optimal control strategy for the WMR with nonholonomic constraints. A nonlinear tracking error model of a mobile robot was linearized by Bahadorian *et al.* [9], [10], and a robust model prediction controller (RMPC) was proposed to perform path tracking control. The guidance of autonomous vehicles was described as an optimal control problem with constraints by Gutjahr *et al.* [11], and a lateral guidance strategy was developed using a linear time-varying MPC method. Plessen and Bemporad [12] designed a linear time-varying predictive control method based on the closed-loop tracking control theory. Li *et al.* [13] proposed an MPC method based on neural-dynamic optimization to achieve the trajectory tracking of a nonholonomic mobile robot. Ali *et al.* [14] linearized the nonlinear behavior of a robot and proposed a hybrid controller based on the fuzzy logic theory, pole placement, and tracking.

The methods based on the first-order Taylor expansion of complex nonlinear systems has obvious advantages for simple applications and the more mature linear control theory can be used to solve the problems rapidly [15]. However, when the higher order terms are ignored, some features of the original system may be lost and the defect is amplified when the errors and continuous random disturbances are large.

With the increasing development of computer technology, some researchers have tried to solve this problem by using nonlinear theory and numerical calculation theory. For example, Park *et al.* [16] proposed an adaptive output-feedback controller in the presence of parametric uncertainties to study the tracking control of nonlinear systems. Chen *et al.* [17] proposed a hierarchical control system structure at three levels (high, low and intermediate) that tracked the autonomous vehicles under the conditions of uncertainty and external disturbances. Ostafew *et al.* [18] proposed a learning-based nonlinear MPC method by modeling the disturbance as a Gaussian process to achieve the path control of a mobile robot. The kinematics, actuator dynamics, and rolling resistance were modeled by Leena and Saju [19], a smooth trajectory tracking controller was designed, and the precise trajectory tracking results were presented. Asif *et al.* [20] put forward a type of output-feedback control using an adaptive sliding mode control theory and analyzed the stability of the observer. Based on the theory of an extreme learning machine and a hybrid chaos optimization algorithm, Yang *et al.* [21] designed a nonlinear predictive control strategy to solve a tracking control problem in the presence of external disturbances. Korayem and Nekoo [22] designed a state-dependent differential Riccati equation (SDDRE) controller for a nonlinear tracking system and obtained suboptimal and feedforward control gain.

Although these methods can largely retain the original system characteristic and the accuracy can be high, the calculation efficiency is relatively low and it is difficult to achieve online tracking control. In addition, the detection of real-time errors and disturbances are often required in engineering practice and this is difficult to achieve. In order to solve this problem, we design an online tracking control method with high precision and computational efficiency. For this purpose, we firstly model the tracking problem of the UGS and convert it into a continuous nonlinear optimal control problem. According to the characteristics of tracking problem, the main purpose is to reduce the deviation between the actual and ideal value of state variables, and [23] designed the method to solve the optimal control problem of path planning for UGS, but the objective function is mainly composed of control variables and time terms. Therefore, on the basis of the previous work, the symplectic pseudospectral method is proposed to solve the optimal control problem, including state variables and control variables in the objective function, combined with the third kind of generation function in this paper, which not only has a high efficiency but also greatly reduces the sensitivity of the initial assumed values of the costate variables. The most obvious characteristic is the introduction of the symplectic theory, which allows the phase flow to maintain the symplectic structure after the discretization. The online optimal tracking control method based on the receding horizon control (RHC) principle and the symplectic pseudospectral method is designed by considering the influences of random disturbances in the environment; a simulation experiment is conducted to verify the proposed method.

II. THE NONLINEAR OPTIMAL CONTROL MODEL OF ERROR

The acceleration of motion control for UGS is provided by the rear wheels, and the orientation is controlled by the front wheels. Assuming that sliding rolling will not occur, the motion can be analyzed without considering the horizontal thrust, friction or inertia characteristics, and a nonholonomic constraint can be obtained as follows,

$$\frac{d}{dt}\begin{pmatrix} x^r \\ y^r \\ \theta^r \end{pmatrix} = \begin{pmatrix} V^r \cos\theta^r \\ V^r \sin\theta^r \\ \omega^r \end{pmatrix} \tag{1}$$

where, $(*)^r$ denotes the values corresponding to standard trajectories, the direction variable θ^r is the angle between the x axis and the longitudinal axis of the UGS, ω^r is the angular velocity of the front wheel. The state variables $\mathbf{X}^r$ includes two coordinates $\left(x^r \ y^r\right)$ and the direction variable θ^r. The control variable $\mathbf{U}^r$ consists of ω^r and translational velocity V^r.

Kanayama *et al.* [24] deduced the nonlinear error model of the UGS based on the geometrical relation in two-dimensional coordinate system:

$$\mathbf{f}(\mathbf{X}) = \frac{d}{dt}\begin{pmatrix} x \\ y \\ \theta \end{pmatrix} = \begin{pmatrix} (\omega^r - u2)y + u1 \\ -(\omega^r - u2)x + V^r \sin\theta \\ u2 \end{pmatrix} \tag{2}$$

where, $\mathbf{X} = \left(x \ y \ \theta\right)^T$ is error state variables, and $\mathbf{U} = \left(u1 \ u2\right)^T$ is error control variables. And the state and control variables should also satisfy the corresponding constraints, which can be expressed as

$$h\left(\mathbf{X} \ \mathbf{U} \ t\right) \leq \mathbf{0} \tag{3}$$

In the case of tracking problems, the minimum tracking error is usually the final goal, but the control process should be stable too. So, the Bolza type cost function can be used as the objective function,

$$J\left(\mathbf{X}(*) \ \mathbf{U}(*) \ t\right) = \frac{1}{2}\int_{t_0}^{t_f}\left(\mathbf{X}^T\mathbf{Q}\mathbf{X} + \mathbf{U}^T\mathbf{R}\mathbf{U}\right)dt \tag{4}$$

where, t_f is the time to reach the goal, t_0 is the departure time, $(\mathbf{Q})_{ns\times ns}$ and $(\mathbf{R})_{nu\times nu}$ are the weight matrix and J is the objective function, ns and nu is the number of state and control variables, respectively.

As the error system is a highly coupled nonlinear system, and it is hard to solve it directly, we can adopt the quasi-linearization method to solve the equation. So, the nonlinear optimal control model can be converted into a series of linear-quadratic optimal control problems (LQOCPS), and the objective function can be expressed as,

$$J^{[k+1]} = \frac{1}{2}\int_{t_0}^{t_f}\left(\left(\mathbf{X}^{[k+1]}\right)^T \mathbf{Q}^{[k+1]}\left(\mathbf{X}^{[k+1]}\right) + \left(\mathbf{U}^{[k+1]}\right)^T \mathbf{R}^{[k+1]}\left(\mathbf{U}^{[k+1]}\right)\right) dt \quad (5)$$

where, $(*)^{[k+1]}$ denotes the value within the $(k+1) - th$ iterations.

The original nonlinear error system can be expressed as

$$\left[\frac{d\mathbf{X}(t)}{dt}\right]^{[k+1]} = \mathbf{A}^{[k]}\mathbf{X}^{[k+1]} + \mathbf{B}^{[k]}\mathbf{U}^{[k+1]} + \mathbf{W}^{[k]} \quad (6)$$

where,

$$\begin{aligned}\mathbf{A}^{[k]} &= \frac{\partial \mathbf{f}\left(\mathbf{X}\ \mathbf{U}\ t\right)}{\partial \mathbf{X}}\Big|_{\mathbf{X}^{[k]},\mathbf{U}^{[k]}}\\ \mathbf{B}^{[k]} &= \frac{\partial \mathbf{f}\left(\mathbf{X}\ \mathbf{U}\ t\right)}{\partial \mathbf{U}}\Big|_{\mathbf{X}^{[k]},\mathbf{U}^{[k]}}\\ \mathbf{W}^{[k]} &= \mathbf{f}^{[k]} - \mathbf{A}^{[k]}\mathbf{X}^{[k]} - \mathbf{B}^{[k]}\mathbf{U}^{[k]}\end{aligned}$$

And constraints can be expressed as

$$\mathbf{C}^{[k]}\mathbf{X}^{[k+1]} + \mathbf{D}^{[k]}\mathbf{U}^{[k+1]} + \mathbf{V}^{[k]} \leq \mathbf{0} \quad (7)$$

where,

$$\begin{aligned}\mathbf{C}^{[k]} &= \frac{\partial \mathbf{h}\left(\mathbf{X}\ \mathbf{U}\ t\right)}{\partial \mathbf{X}}\Big|_{\mathbf{X}^{[k]},\mathbf{U}^{[k]}}\\ \mathbf{D}^{[k]} &= \frac{\partial \mathbf{h}\left(\mathbf{X}\ \mathbf{U}\ t\right)}{\partial \mathbf{U}}\Big|_{\mathbf{X}^{[k]},\mathbf{U}^{[k]}}\\ \mathbf{V}^{[k]} &= \mathbf{h}^{[k]} - \mathbf{C}^{[k]}\mathbf{X}^{[k]} - \mathbf{D}^{[k]}\mathbf{U}^{[k]}\end{aligned}$$

According to the preceding derivation, the results from quasilinearization will not lead to the loss of precision for introducing the $\mathbf{W}^{[k]}$ and $\mathbf{V}^{[k]}$. In order to make it more concise, the iteration designation will be ignored, and

$$\begin{cases}\dot{\mathbf{X}} = \mathbf{AX} + \mathbf{BU} + \mathbf{W}, \quad \mathbf{X}(t_0) = \mathbf{X}_0,\ \mathbf{X}\left(t_f\right) = \mathbf{X}_f\\ \mathbf{CX} + \mathbf{DU} + \mathbf{V} \leq \mathbf{0}\end{cases} \quad (8)$$

The equality of constraints can be obtained by introducing a non-negative slack vector $\boldsymbol{\alpha}$ for the inequality,

$$\mathbf{CX} + \mathbf{DU} + \mathbf{V} + \boldsymbol{\alpha} = \mathbf{0} \quad (9)$$

Then, the optimal control model for path planning is described as

$$\text{Minimize } J = \frac{1}{2}\int_{t_0}^{t_f}\left((\mathbf{X})^{\mathbf{T}}\mathbf{QX} + (\mathbf{U})^{\mathbf{T}}\mathbf{RU}\right)dt$$

$$\text{subject to } \begin{cases}\dot{\mathbf{X}} = \mathbf{AX}+\mathbf{BU}+\mathbf{W}, \quad \mathbf{X}(t_0)=\mathbf{X}_0,\ \mathbf{X}\left(t_f\right)=\mathbf{X}_f\\ \mathbf{CX} + \mathbf{DU} + \mathbf{V} + \boldsymbol{\alpha} = \mathbf{0}\end{cases} \quad (10)$$

And Eq. (10) can be transformed into an unconstrained problem by introducing the Lagrange multiplier vector $\boldsymbol{\lambda}$ and the multiplier vector $\boldsymbol{\beta}$. According to the Pontryagin's maximum principle, the multiplier vector should satisfies $\boldsymbol{\alpha}^{\mathbf{T}}\boldsymbol{\beta} = 0$, and $\boldsymbol{\beta} \geq \mathbf{0}$. So, the objective function can be described as

$$J = \frac{1}{2}\int_{t_0}^{t_f}\left(H - \boldsymbol{\lambda}^{\mathbf{T}}\dot{\mathbf{X}}\right) dt \quad (11)$$

where, the Hamiltonian function is

$$H = \frac{1}{2}\left((\mathbf{X})^{\mathbf{T}}\mathbf{QX} + (\mathbf{U})^{\mathbf{T}}\mathbf{RU}\right) + \boldsymbol{\lambda}^{\mathbf{T}}(\mathbf{AX} + \mathbf{BU} + \mathbf{W}) + \boldsymbol{\beta}^{\mathbf{T}}(\mathbf{CX} + \mathbf{DU} + \mathbf{V} + \boldsymbol{\alpha})$$

According to the classical variational method, if J is minimal, the Hamiltonian system needs to satisfy the control equation, the Hamiltonian canonical equation. And the control equation is

$$\frac{\partial H}{\partial \mathbf{U}} = \mathbf{U} + \mathbf{B}^{\mathbf{T}}\boldsymbol{\lambda} + \mathbf{D}^{\mathbf{T}}\boldsymbol{\beta} = \mathbf{0} \quad (12)$$

Combining Eq. (12) with the Hamiltonian function, and taking the partial derivative of the Hamiltonian function, the Hamiltonian canonical equations can be obtained as follows,

$$\begin{cases}\dot{\mathbf{X}} = \dfrac{\partial H}{\partial \boldsymbol{\lambda}} = \mathbf{AX} - \mathbf{BR}^{-1}\left(\mathbf{B}^T\boldsymbol{\lambda} + \mathbf{D}^T\boldsymbol{\beta}\right) + \mathbf{W}\\ \dot{\boldsymbol{\lambda}} = -\dfrac{\partial H}{\partial \mathbf{X}} = -\mathbf{A}^T\boldsymbol{\lambda} - \mathbf{C}^T\boldsymbol{\beta} - \mathbf{QX}\end{cases} \quad (13)$$

The Hamiltonian function is the function of $\mathbf{X}$, $\mathbf{U}$, $\boldsymbol{\lambda}$, $\boldsymbol{\beta}$ and $\boldsymbol{\alpha}$, and $\mathbf{U}$ can be expressed by $\mathbf{X}$, $\boldsymbol{\lambda}$, $\boldsymbol{\beta}$ and $\boldsymbol{\alpha}$ according to Eq. (12). Thus, H can be viewed as the function of the four independent variables $\mathbf{X}$, $\boldsymbol{\lambda}$, $\boldsymbol{\beta}$ and $\boldsymbol{\alpha}$. And the third kind of generation function within the time interval $\left[a\ b\right]$ is [25]–[27]

$$S = (\boldsymbol{\lambda}_b)^{\mathbf{T}}\mathbf{X}_b + \int_a^b\left(\boldsymbol{\lambda}^{\mathbf{T}}\dot{\mathbf{X}} - H\right) dt \quad (14)$$

According to the Hamiltonian canonical equation, the variation of S is

$$\delta S = (\delta\boldsymbol{\lambda}_a)^{\mathbf{T}}\mathbf{X}_a + (\delta\mathbf{X}_b)^{\mathbf{T}}\boldsymbol{\lambda}_b \quad (15)$$

So, the third kind of generation function is just a function of the state variables at the right end of the interval and costate variables at the left end of the interval.

III. THE SYMPLECTIC PSEUDOSPECTRAL METHOD BASED ON THE THIRD KIND OF GENERATION FUNCTION

A. THE APPROXIMATION OF THE FOUR INDEPENDENT VARIABLES BASED ON THE LEGENDRE PSEUDOSPECTRAL METHOD

The time domain $\Lambda = \left[t_0\ t_f\right]$ can be discretized into P intervals, and the jth interval is $\Lambda^j = \left[t_{j-1}\ t_j\right], j = 1, 2, \cdots, P$. $\forall t \in \Lambda^j$, there is a mapping relations Ξ to realize the transformation from t to $\tau \in \left[-1\ 1\right]$,

$$\Xi : \tau = \frac{2t - (t_j + t_{j-1})}{t_j - t_{j-1}} \quad (16)$$

Then, the following relationship can be obtained,

$$\frac{d\tau}{dt} = \frac{2}{t_j - t_{j-1}} \tag{17}$$

In the next step, the $\mathbf{X}^j$, $\boldsymbol{\lambda}^j$, $\boldsymbol{\beta}^j$ and $\boldsymbol{\alpha}^j$ in the jth interval should be approximated by the N^j order Lagrange interpolating polynomial based on the LGL quadrature nodes, and the LGL nodes τ_l^j, $l = 1, 2, \cdots, N^j - 1$, are the roots of the derivative of the Legendre polynomial $\dot{L}^j(\tau) = 0$. The nodes are located in $[-1\ 1]$, and the $N^j + 1$ LGL nodes are $\left(-1, \tau_1^j, \cdots, \tau_{N^j-2}^j\ 1\right)$ combined with the first nodes $\tau_0^j = -1$ and the last nodes $\tau_{N^j}^j = 1$. The expression of $\mathbf{H\Gamma}^j$ as follows [28]:

$$\mathbf{H\Gamma}^j(\tau) = \sum_{l=0}^{N^j} \mathbf{H\Gamma}_l^j \frac{(\tau^2-1)\dot{L}^j(\tau)}{N^j(N^j+1)\left(\tau - \tau_l^j\right)L_l^j} \tag{18}$$

where, $\mathbf{H\Gamma}^j$ can be $\mathbf{X}^j$, $\boldsymbol{\lambda}^j$, $\boldsymbol{\beta}^j$ and $\boldsymbol{\alpha}^j$, and $(*)_0^j = (*)_{N^{j-1}}^{j-1}$,. $j = 2, 3, \cdots, P$

B. THE APPLICATION OF THE SYMPLECTIC METHOD BASED ON THE THIRD KIND OF GENERATION FUNCTION TO EACH INTERVAL

The derivative of $\mathbf{X}^j(\tau)$ at the LGL node is given by:

$$\frac{d\mathbf{X}_k^j(\tau)}{d\tau} = \sum_{l=0}^{N^j} \mathbf{X}_l^j \mathbf{D}_{kl}^j \tag{19}$$

where, the $(N+1) \times (N+1)$ differentiation matrix $\mathbf{D}_{kl}^j$ is defined as the pseudospectral differential matrix. And the third kind of generation function can be expressed as [29], [30]:

$$\begin{aligned} S\left(\lambda_0^j\ \mathbf{X}_{N^j}^j\right) &= \left(\lambda_0^j\right)^T \mathbf{X}_0^j \\ &+ \sum_{k=0}^{N^j} w_k^j \left[\left(\lambda_k^j\right)^T \sum_{l=0}^{N^j} \mathbf{D}_{kl}^j \mathbf{X}_l^j - \frac{t^j - t^{j-1}}{2} H\right] \end{aligned} \tag{20}$$

where, w_k^j is the weight coefficient of the jth interval, and the expression is

$$w_k^j = \frac{2}{N^j(N^j+1)\left(L_k^j\right)^2} \tag{21}$$

Since the third kind of generation function is just a function of $\boldsymbol{\lambda}_0^j$ and $\mathbf{X}_{N^j}^j$, it can be considered as independent variables, while the others are stationary points of S^j in the jth interval, thus the stationary condition can be applied to them as follows,

$$\begin{cases} \dfrac{\partial S_0^j}{\partial \boldsymbol{\lambda}_0^j} = \mathbf{X}_0^j \\ \dfrac{\partial S_m^j}{\partial \boldsymbol{\lambda}_m^j} = \mathbf{0},\ m = 1, 2, \cdots, N^j \\ \dfrac{\partial S_m^j}{\partial \mathbf{X}_m^j} = \mathbf{0},\ m = 0, 1, \cdots, N^j - 1 \\ \dfrac{\partial S_{N^j}^j}{\partial \mathbf{X}_{N^j}^j} = \boldsymbol{\lambda}_{N^j}^j \end{cases} \tag{22}$$

where,

$$\begin{aligned} \bar{\mathbf{X}}^j &= \left\{\left(\mathbf{X}_0^j\right)^T, \left(\mathbf{X}_1^j\right)^T, \cdots, \left(\mathbf{X}_{N^j-1}^j\right)^T\right\}^T \bar{\boldsymbol{\lambda}}^j \\ &= \left\{\left(\boldsymbol{\lambda}_1^j\right)^T, \left(\boldsymbol{\lambda}_2^j\right)^T, \cdots, \left(\boldsymbol{\lambda}_{N^j}^j\right)^T\right\}^T \end{aligned}$$

And $\frac{\partial S_m^j}{\partial \mathbf{X}_m^j}$, $\frac{\partial S_m^j}{\partial \boldsymbol{\lambda}_m^j}$ can be expressed as

$$\begin{cases} \dfrac{\partial S_m^j}{\partial \boldsymbol{\lambda}_m^j} = \sum\limits_{n=0}^{N^j} \left(\mathbf{K}_{mn}^{\boldsymbol{\lambda\lambda}}\right)^j \boldsymbol{\lambda}_n^j + \sum\limits_{n=0}^{N^j} \left(\mathbf{K}_{mn}^{\boldsymbol{\lambda}X}\right)^j \mathbf{X}_n^j + \left(\boldsymbol{\xi}_m^{\boldsymbol{\lambda}}\right)^j \boldsymbol{\beta}_m^j + \left(\boldsymbol{\gamma}_m^{\boldsymbol{\lambda}}\right)^j \\ \dfrac{\partial S_m^j}{\partial \mathbf{X}_m^j} = \sum\limits_{n=0}^{N^j} \left(\mathbf{K}_{mn}^{\mathbf{X}\boldsymbol{\lambda}}\right)^j \boldsymbol{\lambda}_n^j + \sum\limits_{n=0}^{N^j} \left(\mathbf{K}_{mn}^{\mathbf{XX}}\right)^j \mathbf{X}_n^j + \left(\boldsymbol{\xi}_m^{\mathbf{X}}\right)^j \boldsymbol{\beta}_m^j + \left(\boldsymbol{\gamma}_m^{\mathbf{X}}\right)^j \end{cases} \tag{23}$$

where,

$$\begin{aligned} \left(\mathbf{K}_{mn}^{\boldsymbol{\lambda\lambda}}\right)^j &= \frac{t^j - t^{j-1}}{2} w_m^j \mathbf{B}_m^j \left(\mathbf{B}_m^j\right)^T \delta_m^n \\ \left(\mathbf{K}_{mn}^{\boldsymbol{\lambda}\mathbf{X}}\right)^j &= \left[\left(K_{mn}^{\mathbf{X}\boldsymbol{\lambda}}\right)^j\right]^T \\ &= -w_m^j \mathbf{D}_{mn}^j - \delta_m^0 \delta_m^0 \mathbf{I} - \frac{t^j - t^{j-1}}{2} w_m^j \left(\mathbf{A}_m^j\right)^T \delta_m^n \\ \left(\mathbf{K}_{mn}^{\mathbf{XX}}\right)^j &= (\mathbf{0})_{ns(N^j+1)\times ns(N^j+1)} \\ \left(\boldsymbol{\xi}_m^{\boldsymbol{\lambda}}\right)^j &= \frac{t^j - t^{j-1}}{2} w_m^j \mathbf{B}_m^j \left(\mathbf{D}_m^j\right)^T \\ \left(\boldsymbol{\xi}_m^{\mathbf{X}}\right)^j &= -\frac{t^j - t^{j-1}}{2} w_m^j \left(\mathbf{C}_m^j\right)^T \\ \left(\boldsymbol{\gamma}_m^{\boldsymbol{\lambda}}\right)^j &= -\frac{t^j - t^{j-1}}{2} \mathbf{W}_m^j \\ \left(\boldsymbol{\gamma}_m^{\boldsymbol{\lambda}}\right)^j &= (\mathbf{0})_{ns(N^j+1)\times 1} \end{aligned}$$

Then,

$$\begin{bmatrix} \mathbf{K}_{11}^j & \mathbf{K}_{12}^j & \mathbf{K}_{13}^j & \mathbf{K}_{14}^j \\ \mathbf{K}_{21}^j & \mathbf{K}_{22}^j & \mathbf{K}_{23}^j & \mathbf{K}_{24}^j \\ \mathbf{K}_{31}^j & \mathbf{K}_{32}^j & \mathbf{K}_{33}^j & \mathbf{K}_{34}^j \\ \mathbf{K}_{41}^j & \mathbf{K}_{42}^j & \mathbf{K}_{43}^j & \mathbf{K}_{44}^j \end{bmatrix} \boldsymbol{\sigma}^j + \begin{bmatrix} \boldsymbol{\xi}_{\boldsymbol{\lambda}}^j \\ \boldsymbol{\xi}_{\mathbf{X}}^j \end{bmatrix} \boldsymbol{\beta}^j + \begin{bmatrix} \boldsymbol{\gamma}_{\boldsymbol{\lambda}}^j \\ \boldsymbol{\gamma}_{\mathbf{X}}^j \end{bmatrix} = \begin{bmatrix} \mathbf{X}^{j-1} \\ (\mathbf{0})_{N^j\times 1} \\ (\mathbf{0})_{N^j\times 1} \\ \boldsymbol{\lambda}^j \end{bmatrix} \tag{24}$$

where, the expression of $\boldsymbol{\sigma}^j$ and $\boldsymbol{\beta}^j$ is

$$\begin{cases} \boldsymbol{\sigma}^j = \left\{ (\boldsymbol{\lambda}^{j-1})^T, \left(\bar{\boldsymbol{\lambda}}^j\right)^T, (\bar{\mathbf{X}}^j)^T, (\mathbf{X}^j)^T \right\}^T \\ \boldsymbol{\beta}^j = \left\{ \left(\boldsymbol{\beta}_0^j\right)^T, \left(\boldsymbol{\beta}_1^j\right)^T, \cdots, \left(\boldsymbol{\beta}_{Nj}^j\right)^T \right\}^T \end{cases}$$

The detailed coefficient expressions of σ^j is

$$\mathbf{K}_{11}^j = \left(\mathbf{K}^{\lambda\lambda}\right)^j_{(1:ns)\times(1:ns)}, \mathbf{K}_{12}^j = \left(\mathbf{K}^{\lambda\lambda}\right)^j_{(1:ns)\times(ns+1:end)},$$
$$\mathbf{K}_{13}^j = \left(\mathbf{K}^{\lambda\mathbf{X}}\right)^j_{(1:ns)\times(1:ns)}, \mathbf{K}_{21}^j = \left(\mathbf{K}_{12}^j\right)^T,$$
$$\mathbf{K}_{23}^j = \left(\mathbf{K}^{\lambda\mathbf{X}}\right)^j_{(ns+1:end)\times(1:ns)},$$
$$\mathbf{K}_{24}^j = \left(\mathbf{K}^{\lambda\mathbf{X}}\right)^j_{(ns+1:end)\times(ns+1:end)},$$
$$\mathbf{K}_{31}^j = \left(\mathbf{K}_{13}^j\right)^T, \mathbf{K}_{32}^j = \left(\mathbf{K}_{23}^j\right)^T,$$
$$\mathbf{K}_{33}^j = \left(\mathbf{K}^{\lambda\lambda}\right)^j_{(1:end-ns)\times(1:ns)},$$
$$\mathbf{K}_{34}^j = \left(\mathbf{K}^{\lambda\lambda}\right)^j_{(1:end-ns)\times(ns+1:end)},$$
$$\mathbf{K}_{41}^j = \left(\mathbf{K}_{14}^j\right)^T, \mathbf{K}_{42}^j = \left(\mathbf{K}_{24}^j\right)^T, \mathbf{K}_{43}^j = \left(\mathbf{K}_{34}^j\right)^T.$$

The coefficient matrix of $\boldsymbol{\beta}^j$ is $\boldsymbol{\xi}^j$, the constant matrix term is $\boldsymbol{\gamma}^j$, the right side is $\mathbf{r}^j$, then,

$$\mathbf{K}^j\boldsymbol{\sigma}^j + \boldsymbol{\xi}^j\boldsymbol{\beta}^j + \boldsymbol{\gamma}^j = \mathbf{r}^j \tag{25}$$

The relationships of $\mathbf{U} = \mathbf{g}\left(\mathbf{X}, \boldsymbol{\lambda}, \boldsymbol{\beta}\right)$ can be obtained, and the constraint equation in the jth interval can be organized as

$$\mathbf{C}^j\mathbf{X}^j - \mathbf{H}^j\boldsymbol{\lambda}^j - \mathbf{M}^j\boldsymbol{\beta}^j + \mathbf{V}^j + \boldsymbol{\alpha}^j = 0 \tag{26}$$

where, the detailed coefficient expressions of $\mathbf{X}^j$, $\boldsymbol{\lambda}^j$, $\boldsymbol{\beta}^j$ are

$$\begin{cases} \mathbf{C}^j = diag\left(\mathbf{C}_0^j, \mathbf{C}_1^j, \cdots, \mathbf{C}_{Nj}^j\right) \\ \mathbf{H}^j = diag\left\{\mathbf{D}_0^j\left(\mathbf{B}_0^j\right)^T, \mathbf{D}_1^j\left(\mathbf{B}_1^j\right)^T, \cdots, \mathbf{D}_{Nj}^j\left(\mathbf{B}_{Nj}^j\right)^T\right\} \\ \mathbf{M}^j = diag\left\{\mathbf{D}_0^j\left(\mathbf{D}_0^j\right)^T, \mathbf{D}_1^j\left(\mathbf{D}_1^j\right)^T, \cdots, \mathbf{D}_{Nj}^j\left(\mathbf{D}_{Nj}^j\right)^T\right\} \end{cases}$$

and

$$\mathbf{V}^j = \left\{ \left(\mathbf{V}_0^j\right)^T, \left(\mathbf{V}_1^j\right)^T, \cdots, \left(\mathbf{V}_{Nj}^j\right)^T \right\}^T$$
$$\boldsymbol{\alpha}^j = \left\{ \left(\boldsymbol{\alpha}_0^j\right)^T, \left(\boldsymbol{\alpha}_1^j\right)^T, \cdots, \left(\boldsymbol{\alpha}_{Nj}^j\right)^T \right\}^T$$

Accordingly, the compact formula of the jth interval is

$$\begin{cases} \mathbf{K}^j\boldsymbol{\sigma}^j + \boldsymbol{\xi}^j\boldsymbol{\beta}^j + \boldsymbol{\gamma}^j = \mathbf{r}^j \\ \boldsymbol{\Gamma}^j\boldsymbol{\sigma}^j - \mathbf{M}^j\boldsymbol{\beta}^j + \mathbf{V}^j + \boldsymbol{\alpha}^j = \mathbf{0} \\ \left(\boldsymbol{\alpha}^j\right)^T \boldsymbol{\beta}^j = 0, \quad \boldsymbol{\alpha}^j \geq \mathbf{0}, \boldsymbol{\beta}^j \geq \mathbf{0} \end{cases} \tag{27}$$

where, $\boldsymbol{\Gamma}^j = [-\mathbf{H}^j, \mathbf{C}^j]$.

C. THE RESULT OF THE WHOLE-TIME DOMAIN

The compact form can be obtained by assembling the result of each interval in the whole-time domain as follows,

$$\begin{cases} \mathbf{K}\boldsymbol{\sigma} + \boldsymbol{\xi}\boldsymbol{\beta} + \boldsymbol{\gamma} = \mathbf{r} \\ \boldsymbol{\Gamma}\boldsymbol{\sigma} - \mathbf{M}\beta + \mathbf{V} + \boldsymbol{\alpha} = \mathbf{0} \\ (\boldsymbol{\alpha})^T \boldsymbol{\beta} = 0, \quad \boldsymbol{\alpha} \geq \mathbf{0}, \boldsymbol{\beta} \geq \mathbf{0} \end{cases} \tag{28}$$

where, the coefficient $\mathbf{K}$ is a sparse and symmetric matrix, and the coefficient matrixes of Eq. (28) are

$$\mathbf{K} = \begin{bmatrix} \mathbf{K}^1 & \mathbf{Z}^1 & & & \\ (\mathbf{Z}^1)^T & \mathbf{K}^2 & \mathbf{Z}^2 & & \\ & (\mathbf{Z}^2)^T & \ddots & \mathbf{Z}^{P-1} \\ & & (\mathbf{Z}^{P-1})^T & \mathbf{K}^P \end{bmatrix}$$

$$\mathbf{Z}^j = \begin{bmatrix} \mathbf{0}_{(2ns\times N^j+ns)\times ns} & \mathbf{0}_{(2ns\times N^j+ns)\times(2ns\times N^j+ns)} \\ -\mathbf{I}_{ns\times ns} & \mathbf{0}_{ns\times(2ns\times N^j+ns)} \end{bmatrix}$$

$$\begin{cases} \boldsymbol{\xi} = diag\left(\boldsymbol{\xi}^1, \boldsymbol{\xi}^2, \cdots, \boldsymbol{\xi}^P\right) \\ \boldsymbol{\Gamma} = diag\left(\boldsymbol{\Gamma}^1, \boldsymbol{\Gamma}^2, \cdots, \boldsymbol{\Gamma}^P\right) \\ \mathbf{M} = diag\left(\mathbf{M}^1, \mathbf{M}^2, \cdots, \mathbf{M}^P\right) \end{cases}$$

The constant matrix terms are

$$\begin{cases} \boldsymbol{\gamma} = \left\{ (\boldsymbol{\gamma}^1)^T, (\boldsymbol{\gamma}^2)^T, \cdots, (\boldsymbol{\gamma}^P)^T \right\}^T \\ \mathbf{r} = \left(\mathbf{X}_0, \mathbf{0}_{1\times sd}, \boldsymbol{\lambda}_f\right)^T \\ \mathbf{V} = \left\{ (\mathbf{V}^1)^T, (\mathbf{V}^2)^T, \cdots, (\mathbf{V}^P)^T \right\}^T \\ \boldsymbol{\alpha} = \left\{ (\boldsymbol{\alpha}^1)^T, (\boldsymbol{\alpha}^2)^T, \cdots, (\boldsymbol{\alpha}^P)^T \right\}^T \end{cases}$$

where, $sd = \sum_{k=1}^{P} 2ns\left(N^j + 1\right) - 2ns$, and

$$\begin{cases} \mathbf{X} = \left\{ (\mathbf{X}^1)^T, (\mathbf{X}^2)^T, \cdots, (\mathbf{X}^P)^T \right\}^T \\ \lambda = \left\{ (\lambda^1)^T, (\lambda^2)^T, \cdots, (\lambda^P)^T \right\}^T \\ \boldsymbol{\beta} = \left\{ \left(\boldsymbol{\beta}^1\right)^T, \left(\boldsymbol{\beta}^2\right)^T, \cdots, (\boldsymbol{\beta}^P)^T \right\}^T \\ \boldsymbol{\sigma} = \left\{ (\boldsymbol{\sigma}^1)^T, (\boldsymbol{\sigma}^2)^T, \cdots, (\boldsymbol{\sigma}^P)^T \right\}^T \end{cases}$$

Considering the boundary conditions $\mathbf{X}_0$ and $\mathbf{X}_f$, the relevant matrix need to be modified as follows,

(1). The elements in the row $ns\left(N^1 + 1\right) + 1 : ns\left(N^1 + 2\right)$ of $\mathbf{K}$, $\boldsymbol{\xi}$ and $\boldsymbol{\gamma}$ are replaced with 0, the sections of columns $ns\left(N^1 + 1\right) + 1 : ns\left(N^1 + 2\right)$ and rows $ns\left(N^1 + 1\right) + 1 : ns\left(N^1 + 2\right)$ are replaced with the unit matrix, the rows $ns\left(N^1 + 1\right) + 1 : ns\left(N^1 + 2\right)$ of $\mathbf{r}$ are replaced with $\mathbf{X}_0$;

(2). The elements in the last ns rows of $\mathbf{K}$, $\boldsymbol{\xi}$ and $\boldsymbol{\gamma}$ are replaced with 0, the sections of the last ns columns and the last ns rows of $\mathbf{K}$ are replaced with the unit matrix, and the last ns rows of $\mathbf{r}$ are replaced with $\mathbf{X}_f$.

The state variables and covariates can be obtained as follows,

$$\boldsymbol{\sigma} = -\mathbf{K}^{-1}\boldsymbol{\xi}\boldsymbol{\beta} - \mathbf{K}^{-1}\left(\boldsymbol{\gamma} - \mathbf{r}\right) \tag{29}$$

Thus, the optimal control solution can be obtained by the following relationship.

$$\begin{cases} \mathbf{Y}\beta + \mathbf{q} = \boldsymbol{\alpha} \\ (\boldsymbol{\alpha})^T \boldsymbol{\beta} = 0, \quad \boldsymbol{\alpha} \geq \mathbf{0},\ \boldsymbol{\beta} \geq \mathbf{0} \end{cases} \tag{30}$$

where, $\mathbf{Y} = \boldsymbol{\Gamma}\mathbf{K}^{-1}\boldsymbol{\xi} + \mathbf{M}$, $\mathbf{q} = \boldsymbol{\Gamma}\mathbf{K}^{-1}(\boldsymbol{\gamma} - \mathbf{r}) - \mathbf{V}$.

Since the $\boldsymbol{\beta}$ and $\boldsymbol{\alpha}$ satisfy the orthogonality relationship, the Lemke method is adopted to obtain the $\boldsymbol{\beta}$ and $\boldsymbol{\alpha}$ in this paper, and the optimal control $\mathbf{U} = \mathbf{g}(\mathbf{X}, \boldsymbol{\lambda}, \boldsymbol{\beta})$ can also be obtained. Thus, the optimal control question is completely solved.

IV. THE ONLINE OPTIMAL TRACKING CONTROL METHOD BASED ON RHC

A. THE BOUNDARY CONDITIONS OF THE TIME WINDOW

Assuming the length of the sliding time window is T and the window is $\Delta_k = [t^0_{\Delta k}\ t^0_{\Delta k} + T]$. At $k = 1$, the initial error $\mathbf{X}^0$ can be regarded as the initial state variable $\mathbf{X}^0_{\Delta 1}$ of the nonlinear error model in the first window.

When $k > 1$, the state variables $\mathbf{X}^0_{\Delta k}$ at $t^0_{\Delta k}$ denote the difference between the actual state variables $\mathbf{X}^a_k$ and the standard state variables $\mathbf{X}^r_k$; the actual error contains two parts: the first part is caused by the error during the preorder moment and it can be calculated within the time window $\Delta_{k-1} = [t^0_{\Delta k-1}\ t^0_{\Delta k-1} + T]$; the second part is the disturbance caused by the equipment, measurement errors, or other random factors at $t^0_{\Delta k}$, which is described by white noise or colored noise.

The first part is only caused by the initial value $\mathbf{X}^0_{\Delta k-1}$ within Δ_{k-1} without considering the disturbance $\mathbf{w}_k$ at $t^0_{\Delta k}$. When the time window is increased $\Delta_k = [t^0_{\Delta k}\ t^0_{\Delta k} + T]$, we have to calculate and measure the actual error state variable at $t^0_{\Delta k}$; it should be used as the left side of the boundary value in the window Δ_k. Therefore, it can be denoted as:

$$\mathbf{X}^0_{\Delta k} = \mathbf{X}^1_{\Delta k-1} + \mathbf{w}_k \tag{31}$$

Because the optimal control is designed to eliminate or reduce the error as far as possible, the final error of the time window can be regarded as $\mathbf{X}^f_{\Delta k} = \mathbf{0}$ and the deviation caused by $\mathbf{X}^0_{\Delta k}$ can be eliminated within Δ_k. Therefore, the right side of the boundary value is $\mathbf{0}$.

Above all, the original problem can be transformed into an optimal control problem in different time windows with a fixed boundary and a fixed time interval. The online tracking can also be achieved by sliding the time window and by solving the optimal control problem in each time window.

B. THE FRAME OF THE ONLINE OPTIMAL TRACKING CONTROL METHOD BASED ON RHC

Based on the above ideas, the online optimal tracking control method based on the RHC can be designed according to the framework as shown in Fig. 1.

The specific steps are as follows,

1) Initialize the time window length parameter T, the sliding time window parameter $k = 1$, and the corresponding boundary of the first time window $\mathbf{X}^0_{\Delta 1} = \mathbf{X}^0$, $\mathbf{X}^f_{\Delta 1} = \mathbf{0}$;
2) Initialize the parameters of the symplectic pseudospectral method, where the number of LGL points is $N + 1$ and the corresponding boundary of the time window $\Delta_k = [t^0_{\Delta k}\ t^0_{\Delta k} + T]$ is $\mathbf{X}^0_{\Delta k}$, $\mathbf{X}^f_{\Delta k} = \mathbf{0}$;
3) Initialize the initial reference solution at each iteration for the symplectic pseudospectral method. For the $u-th$ iteration ($u \geq 1$), if $u = 1$, the initial reference solution $\mathbf{X}^{[0]}_{\Delta k}$, $\mathbf{U}^{[0]}_{\Delta k}$, $\boldsymbol{\lambda}^{[0]}_{\Delta k}$ is generated randomly or the initial reference solution is obtained from the results of the last iteration;
4) Use the symplectic pseudospectral method for iteration. Obtain the optimal control variables set $(\mathbf{U}^0_{\Delta k}, \mathbf{U}^1_{\Delta k}, \cdots \mathbf{U}^N_{\Delta k})$, state variables set $(\mathbf{X}^0_{\Delta k}, \mathbf{X}^1_{\Delta k}, \cdots \mathbf{X}^f)$, and the corresponding time set $(t^0_{\Delta k}, t^1_{\Delta k}, \cdots t^f)$ in time window Δ_k; record and output the result $\mathbf{U}^0_{\Delta k}$, $\mathbf{X}^0_{\Delta k}$, $t^0_{\Delta k}$;
5) Determine the sliding time window, where the initial time and state of the current time window are the second value of the corresponding time set and the corresponding state variable of the last time window respectively; in order to consider the influence of random disturbances, the disturbance is added to the initial state variable of the current time window;
6) If $t^0_{\Delta k+1} + T \geq t_f$, stop the sliding time window and exit the program; otherwise, return step 2) continues the loop.

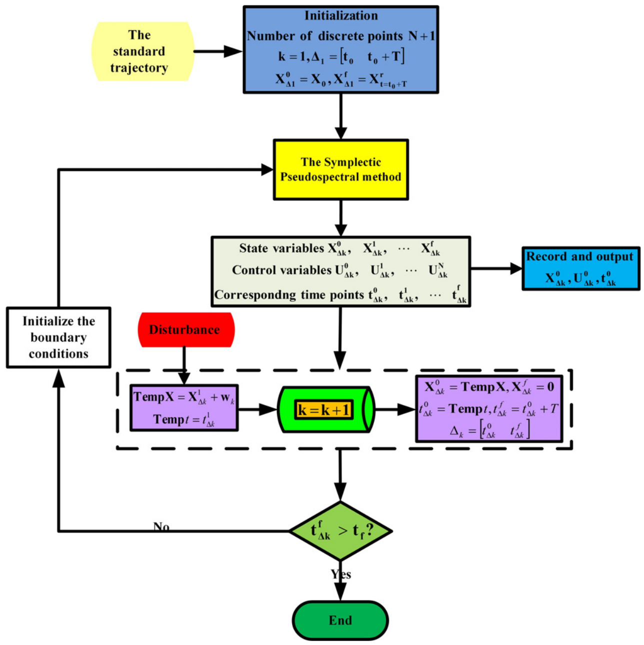

FIGURE 1. The frame of the online tracking optimal control method based on RHC.

V. RESULTS

In order to verify the accuracy and computational efficiency of the online tracking method proposed in this paper, a standard trajectory $\mathbf{X}^r$ and corresponding control $\mathbf{U}^r$ are used for the simulation experiments. The computing environment is Windows 7 64-bit, RAM 4.00 GB, MATLAB R2017a.

A. THE RELATIONSHIP BETWEEN THE STATE VARIABLES AND WEIGHT MATRIX

Because the weight matrix in the objective function reflects the importance of each variable, different results may occur. In order to evaluate this outcome, the importance of the three state variables is assumed to be the same. Because the position of the UGS is only determined by the abscissa, ordinate, and direction angle, the assumption is reasonable and the state variable weight matrix is $\mathbf{Q} = diag\begin{pmatrix}1 & 1 & 1\end{pmatrix}$. In the case of two control variables, the importance can be assumed to be the same, namely, the weight matrix is $\mathbf{R} = diag\begin{pmatrix}1 & 1\end{pmatrix}$.

The coefficient $\boldsymbol{\tau}$ is used to adjust the importance of the state relative to the control variables; the value of $\mathbf{R}$ does not change and $\mathbf{Q}$ is multiplied by the coefficient τ. To describe the effects of different values of $\boldsymbol{\tau}$, an experiment is conducted. The initial setup is: $\mathbf{X}^0 = \begin{pmatrix}0.1 & 0.8 & -0.5\end{pmatrix}^T$, $\mathbf{X}^f = \begin{pmatrix}0.0 & 0.0 & 0.0\end{pmatrix}^T$, $t_0 = 0.0s$, $t_f = 192.76s$, and random disturbances are ignored. The time domain is divided into 20 intervals and each interval is divided into 20 sections in the simulation experiment. The values of τ are 1, 0.1, 0.01, and 0.001. The specific results are as follows.

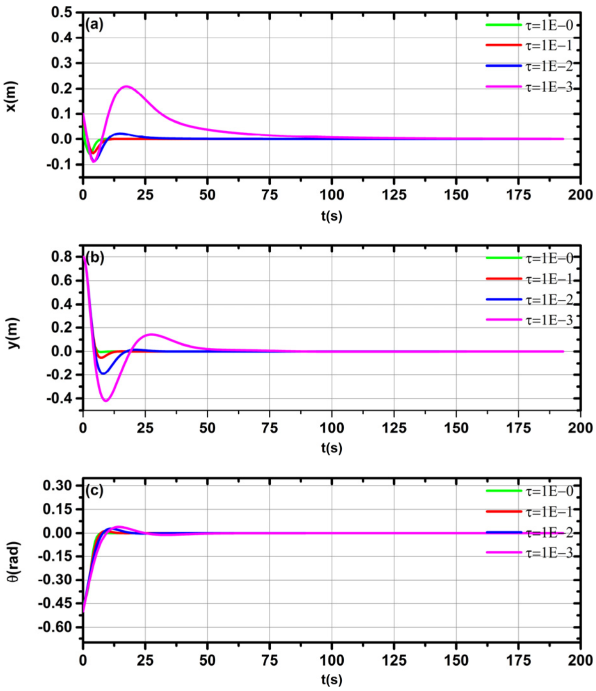

FIGURE 2. **The relationship between the state variables over time under different τ.**

Figure 2 (a), (b), and (c) represents the relationship between the three error state variables over time for different coefficients. A comparative analysis of the results shown in Fig. 2 and the specific calculation results indicates that it takes only 6.3s to reach the level of 10^{-3} with $\tau = 1$, 11.7s with $\tau = 0.1$, 24.8s with $\tau = 0.01$, and 87.4s with $\tau = 0.001$. As the coefficient decreases, the importance of the state variables decreases and the settling-time and overshoot of the state variables increase.

B. TRACKING EXPERIMENT

The principle of this simulation experiment can be expressed as follows, (1) the time interval of the sliding time window is about 1s; (2) the error caused by the initial moment in the time window is basically eliminated with the level of 10^{-3}. According to the results and the principle, the length $T = 12s$ and $\tau = 0.1$.

As the existence of disturbances in the real world, the actual trajectory cannot be exactly coincident with the standard trajectory, and the deviation between the actual trajectory and the standard trajectory is inevitable, a buffer area (to expand the actual contour of the obstacle) should be adopted for obstacle avoidance when the standard trajectory is being calculated. In other words, there is deviation between the actual trajectory and the standard trajectory within a certain range. So, the state should be constrained to ensure that the deviation will be located within a certain range, and the range is predetermined when the standard trajectory is being calculated. The constraints of state and control variables in this simulation experiment are

$$\begin{cases} x^2 + y^2 \le 1 \\ V^r \cos(\theta) - u1 \le 1.1 \\ |u2| \le 0.3 \end{cases}$$

where, the first constraint denotes that the deviation of trajectory will be constrained as $\begin{bmatrix}0 & 1\end{bmatrix}$, the second constraint denotes that the actual linear speed of UGS is no more than 1.1m/s, and the third constraint denotes that the deviation of angular speed will be constrained as $\begin{bmatrix}-0.3 & 0.3\end{bmatrix}$.

The random disturbance is selected as being 0.1 times of the standard Gaussian white noise and $\mathbf{X}^0 = \begin{pmatrix}0.06 & 1 & -0.6\end{pmatrix}^T$. The symplectic pseudospectral method uses a nested grid; the time window is divided into 4 intervals and each interval is divided into 3 segments, $N = 12$. The specific results are shown below.

Figure 3(a) shows the results with the added noise, Fig. 3(b) shows the error state variables based on the error model, it denotes that the state error is located within the range of constraints. What's more, the results are consistent with the constraint of horizontal and vertical axes ($x^2+y^2 \le 1$), which is very important in engineering practice, and it can make sure that the real path will not collision with the obstacles by using the tracking method.

Even though the continuous disturbances occurs in the environment, the online control is achieved to ensure the tracking precision by the method proposed in this paper; it also implies that the control strategy obtained by the method is capable of anti-interference. In order to further test the validity of the results, the control variables can be obtained as follows,

According to the Fig. 4, the actual linear speed of UGS is less than 1.1m/s, and the actual angular speed is located at $\begin{bmatrix}-0.3 & 0.3\end{bmatrix}$, it proved that the results can satisfy

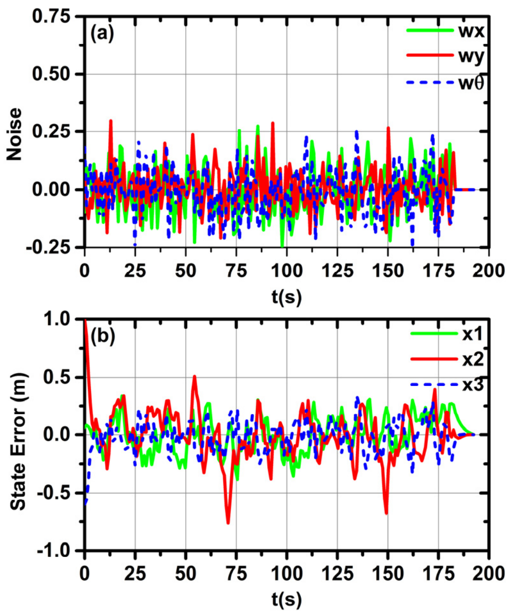

FIGURE 3. Noise and state error of the simulation experiment.

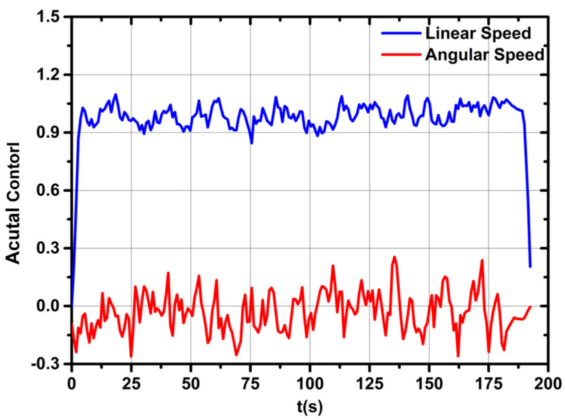

FIGURE 4. Actual linear velocity and angular velocity.

the constraints. So, the proposed method can solve the constrained-state and constrained-control tracking problem. To analyze the tracking accuracy and computational efficiency, the comparison of standard path and actual path will be made as follows,

Fig. 5 shows the standard path and actual path obtained by the proposed method. According to the results, the actual path almost overlaps with the standard path, and the tracking error at the terminal position is 0, which can further prove that the tracking results obtained by this method are of good precision. What's more, it indicates that the method can also be applied in practice with high requirements on terminal posture, such as the parking problem and the trajectory tracking for carrier aircraft on flight deck.

In addition, the interval of the sliding time window is 0.8292s and for 219 sliding time windows, the time required is 8.168s. Each calculation requires 0.0373s, which represents only 4.4983% of the interval. It demonstrates that the proposed method possesses the advantages of fast calculation and can be used for real-time and online tracking.

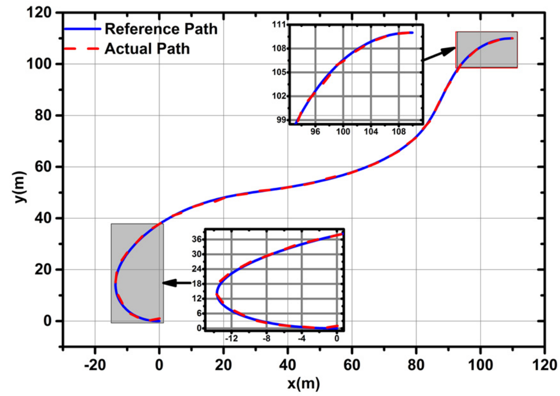

FIGURE 5. The standard path and actual path.

Even though the errors are nonlinear with random disturbances, the online optimal tracking control method based on the RHC achieves online and real-time standard trajectory tracking control and can be used in engineering practice.

VI. CONCLUSIONS

The tracking of a UGS is converted to a continuous nonlinear optimal control problem based on a nonlinear error model and the characteristic of a Hamiltonian system. In order to solve the problem, the symplectic pseudospectral method is proposed. Subsequently, an online optimal tracking control method based on the RHC is presented. Finally, the proposed method is verified using a specific simulation experiment. The results shows that the method has obvious advantages as follows,

(1) It can solve the optimal problems with an infinite-horizon discounted cost, and it can avoid solving the algebraic Riccati equation (ARE) while the traditional methods are hard to avoid it.

(2) The tracking precision is an important aspect of a tracking method, and the real trajectory must not collision with the obstacles for UGS. So, the control and state should be constrained. However, the traditional tracking methods are difficult to solve the tracking problem with inequality constraint of control and state simultaneously. And it can be solved by the method in this paper, and the tracking precision is high.

(3) It eliminates the disadvantages of the traditional nonlinear optimal control method, and reduces the sensitivity to the initial reference solution and the covariates.

(4) The calculation efficiency of this method is very high, which can achieve the purpose of real-time tracking. Moreover, the RHC theory compensates for the disadvantage that the symplectic pseudospectral method is not applicable to online computing. It can be used for online and real-time tracking control of the standard trajectory with disturbances, and it also shows a good ability to adjust the control strategy depending on the actual situation.

In order to improve the efficiency of the algorithm, the framework of the algorithm needs to be further optimized in future work. What's more, if the parameters in weight matrix **Q** can be smaller or the parameters in **R** are larger, it will increase the importance of control variables, and control variables will be smoother too, but it will increase the risk of larger errors. To find the balance, it needs to be further studied. And it's another challenging work to keep balance the relationships of calculation efficiency, accuracy requirements and other engineering requirements, and it will be discussed in future work.

REFERENCES

[1] D. Huang and J. Zhai, "Trajectory tracking of wheeled mobile robots based on disturbance observer," in *Proc. Chin. Automat. Congr.*, Wuhan, China, Nov. 2015, pp. 1761–1765.

[2] A. Zdešar, I. Škrjanc, and G. Klančar, "Visual trajectory-tracking model-based control for mobile robots," *Int. J. Adv. Robot. Syst.*, vol. 10, pp. 1–12, 2013, doi: 10.5772/56757.

[3] S.-M. Lee, H. Kim, S. Lee, and H. Myung, "Nash equilibrium-based geometric pattern formation control for nonholonomic mobile robots," *Adv. Robot. Res.*, vol. 1, no. 1, pp. 41–59, 2014.

[4] C. Y. Sosa-Cervantes, R. Silva-Ortigoza, C. Márquez-Sánchez, H. Taud, and G. Saldaña-González, "Trajectory tracking task in wheeled mobile robots: A review," in *Proc. Int. Conf. Mechatronics, Electron. Automot. Eng.*, Cuernavaca, Mexico, Nov. 2014, pp. 110–115.

[5] P. Falcone, M. Tufo, F. Borrelli, J. Asgari, and H. E. Tseng, "A linear time varying model predictive control approach to the integrated vehicle dynamics control problem in autonomous systems," in *Proc. 46th IEEE Conf. Decis. Control*, New Orleans, LA, USA, Dec. 2007, pp. 2980–2985.

[6] F. Borrelli, P. Falcone, T. Keviczky, J. Asgari, and D. Hrovat, "MPC-based approach to active steering for autonomous vehicle systems," *Int. J. Vehicle Auton. Syst.*, vol. 3, no. 2, pp. 265–291, 2005.

[7] P. Falcone, F. Borrelli, J. Asgari, H. E. Tseng, and D. Hrovat, "Predictive active steering control for autonomous vehicle systems," *IEEE Trans. Control Syst. Technol.*, vol. 15, no. 3, pp. 566–580, May 2007.

[8] F. Kühne, W. F. Lages, and J. M. G. da Silva, Jr., "Model predictive control of a mobile robot using linearization," in *Proc. Mechatronics Robot.*, 2004, pp. 525–530.

[9] M. Bahadorian, R. Eaton, T. Hesketh, and B. Savkovic, "Robust time-varying model predictive control with application to mobile robot unmanned path tracking," *IFAC Proc. Volumes*, vol. 47, no. 3, pp. 4849–4854, 2014.

[10] M. Bahadorian, B. Savkovic, R. Eaton, and T. Hesketh, "Robust model predictive control for automated trajectory tracking of an unmanned ground vehicle," in *Proc. Amer. Control Conf.*, Montreal, QC, Canada, Jun. 2012, pp. 4251–4256.

[11] B. Gutjahr, L. Gröll, and M. Werling, "Lateral vehicle trajectory optimization using constrained linear time-varying MPC," *IEEE Trans. Intell. Transp. Syst.*, vol. 18, no. 6, pp. 1586–1595, Jun. 2017.

[12] M. M. G. Plessen and A. Bemporad, "Reference trajectory planning under constraints and path tracking using linear time-varying model predictive control for agricultural machines," *Biosyst. Eng.*, vol. 153, pp. 28–41, Jan. 2017.

[13] Z. Li, J. Deng, R. Lu, Y. Xu, J. Bai, and C.-Y. Su, "Trajectory-tracking control of mobile robot systems incorporating neural-dynamic optimized model predictive approach," *IEEE Trans. Syst., Man, Cybern., Syst.*, vol. 46, no. 6, pp. 740–749, Jun. 2016.

[14] Z. A. Ali, D. Wang, M. Safwan, W. Jiang, and M. Shafiq, "Trajectory tracking of a nonholonomic wheeleed mobile robot using hybrid controller," *Int. J. Model. Optim.*, vol. 6, no. 3, pp. 136–141, 2016.

[15] Y.-Q. Han and H.-S. Yan, "Adaptive multi-dimensional Taylor network tracking control for SISO uncertain stochastic non-linear systems," *IET Control Theory Appl.*, vol. 12, no. 8, pp. 1107–1115, 2018.

[16] B. S. Park, S. J. Yoo, J. B. Park, and Y. H. Choi, "Adaptive output-feedback control for trajectory tracking of electrically driven non-holonomic mobile robots," *IET Control Theory Appl.*, vol. 5, no. 6, pp. 830–838, Apr. 2011.

[17] C. Chen, Y. Jia, M. Shu, and Y. Wang, "Hierarchical adaptive path-tracking control for autonomous vehicles," *IEEE Trans. Intell. Transp. Syst.*, vol. 16, no. 5, pp. 2900–2912, Oct. 2015.

[18] C. J. Ostafew, A. P. Schoellig, T. D. Barfoot, and J. Collier, "Learning-based nonlinear model predictive control to improve vision-based mobile robot path tracking," *J. Field Robot.*, vol. 33, no. 1, pp. 133–152, 2015.

[19] N. Leena and K. K. Saju, "Modelling and trajectory tracking of wheeled mobile robots," *Procedia Technol.*, vol. 24, pp. 538–545, 2016, doi: 10.1016/j.protcy.2016.05.094.

[20] M. Asif, A. Y. Memon, and M. J. Khan, "Output feedback control for trajectory tracking of wheeled mobile robot," *Intell. Automat. Soft Comput.*, vol. 22, no. 1, pp. 75–87, 2016.

[21] Y. Yang, X. Lin, Z. Miao, X. Yuan, and Y. Wang, "Predictive control strategy based on extreme learning machine for path-tracking of autonomous mobile robot," *Intell. Automat. Soft Comput.*, vol. 21, no. 1, pp. 1–19, 2015.

[22] M. H. Korayem and S. R. Nekoo, "Suboptimal tracking control of nonlinear systems via state-dependent differential Riccati equation for robotic manipulators," in *Proc. 3rd RSI Int. Conf. Robot. Mechatronics*, Tehran, Iran, Oct. 2015, pp. 025–030.

[23] J. Liu, W. Han, C. Liu, and H. Peng, "A new method for the optimal control problem of path planning for unmanned ground systems," *IEEE Access*, vol. 6, pp. 33251–33260, 2018, doi: 10.1109/ACCESS.2018.2846769.

[24] Y. Kanayama, Y. Kimura, F. Miyazaki, and T. Noguchi, "A stable tracking control method for an autonomous mobile robot," in *Proc. IEEE Int. Conf. Robot. Automat.*, Osaka, Japan, Nov. 1991, pp. 384–389.

[25] C. Park and D. J. Scheeres, "A generating function for optimal feedback control laws that satisfies the general boundary conditions of a system," in *Proc. Amer. Control Conf.*, Boston, MA, USA, 2004, pp. 679–684.

[26] C. Park, V. M. Guibout, and D. J. Scheeres, "Solving optimal continuous thrust rendezvous problems with generating functions," *J. Guid., Control, Dyn.*, vol. 37, no. 29, pp. 396–401, 2006.

[27] C. Park and D. J. Scheeres, "Solutions of the optimal feedback control problem using Hamiltonian dynamics and generating functions," in *Proc. 42nd IEEE Int. Conf. Decis. Control*, Maui, HI, USA, Dec. 2003, pp. 1222–1227.

[28] I. M. Ross and F. Fahroo, "Legendre pseudospectral approximations of optimal control problems," in *New Trends in Nonlinear Dynamics and Control and Their Applications*, vol. 295. Berlin, Germany: Springer, 2004, doi: 10.1007/978-3-540-45056-6_21.

[29] H. Peng, Q. Gao, Z. Wu, and W. Zhong, "Symplectic approaches for solving two-point boundary-value problems," *J. Guid., Control, Dyn.*, vol. 35, no. 2, pp. 653–659, 2012.

[30] H. Peng, Q. Gao, Z. Wu, and W. Zhong, "Efficient sparse approach for solving receding-horizon control problems," *J. Guid., Control, Dyn.*, vol. 36, no. 6, pp. 1864–1872, 2013.

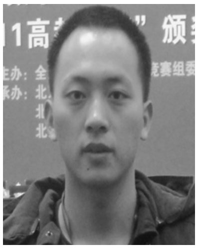

JIE LIU received the M.S. degree from AUAF, China, in 2015. He is currently pursuing the Ph.D. degree with Naval Aeronautical and Astronautical University. His research interests include the control of unmanned ground systems, path planning for robots, and optimal control, and related fields, such as the process industry control and automation.

WEI HAN received the Ph.D. degree from the Nanjing University of Aeronautics and Astronautics, China, in 2003. He is currently a Professor with Naval Aeronautical and Astronautical University, China. His research interests cover the general area of the process industry control and automation, and related fields such as aerodynamics.

YONG ZHANG received the M.S. degree from Naval Aeronautical and Astronautical University, China, in 2008. He is currently with Naval Aeronautical and Astronautical University. His research interests cover the general area of the process industry control and automation, and related fields such as aerodynamics.

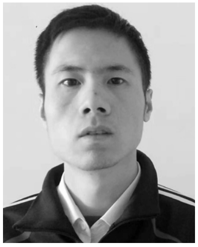

ZHIGANG CHEN received the Ph.D. degree from Naval Aeronautical and Astronautical University, China, in 2018. He is currently an Engineer with the China Aerodynamics Research and Development Center, China. His research interests cover the general area of control and automation, and related fields such as aerodynamics.

HAIJUN PENG received the Ph.D. degree from the Dalian University of Technology, China, in 2012. He is currently an Associate Professor with the State Key Laboratory of Structural Analysis for Industrial Equipment, Department of Engineering Mechanics, Dalian University of Technology. His research interests cover the optimal control, multibody dynamics, and robot system.